J Mater Sci: Mater Med (2010) 21:1495–1502
DOI 10.1007/s10856-010-4000-1

Hydroxyapatite scaffolds processed using a TBA-based freeze-gel casting/polymer sponge technique

Tae Young Yang · Jung Min Lee · Seog Young Yoon · Hong Chae Park

Received: 6 November 2009 / Accepted: 9 January 2010 / Published online: 23 January 2010

Abstract A novel freeze-gel casting/polymer sponge technique has been introduced to fabricate porous hydroxyapatite scaffolds with controlled "designer" pore structures and improved compressive strength for bone tissue engineering applications. Tertiary-butyl alcohol (TBA) was used as a solvent in this work. The merits of each production process, freeze casting, gel casting, and polymer sponge route were characterized by the sintered microstructure and mechanical strength. A reticulated structure with large pore size of 180–360 μm, which formed on burnout of polyurethane foam, consisted of the strut with highly interconnected, unidirectional, long pore channels ($\sim$4.5 μm in dia.) by evaporation of frozen TBA produced in freeze casting together with the dense inner walls with a few, isolated fine pores (<2 μm) by gel casting. The sintered porosity and pore size generally behaved in an opposite manner to the solid loading, i.e., a high solid loading gave low porosity and small pore size, and a thickening of the strut cross section, thus leading to higher compressive strengths.

1 Introduction

The scaffolding materials must satisfy biological requirements such as biocompatibility, bioactivity and osteoconductivity. Among such materials, a calcium phosphate, hydroxyapatite (HA) having a similar chemical composition to the major inorganic component of natural bone is biocompatible and osteoconductive [1–3]. Therefore, HA is undoubtedly accepted as a potential candidate bioceramic insert material for creating bone tissue engineering scaffolds, due to its excellent chemical and biological affinity with bone tissue. Also, the scaffolds require a three-dimensional (3D) interconnected pore structure with a desirable pore size (e.g. 5–15 μm for fibroblasts, 20–125 μm for adult mammalian skin tissues and 100–350 μm for bone tissues) to permit cell infiltration and host tissue ingrowth [4]. The structural properties of scaffolds are mainly determined by the processing technique applied; in this case, the approach to designing novel pore microstructures with high strength sufficient to handle scaffolds and to support their skeleton structure in the initial stage of tissue attachment must be considered.

Several processing routes for fabricating porous bioceramic scaffolds have been developed, including replication of polymer foams [5–7], gel casting of foams [8, 9] and pyrolysis of volatile organic phases [10, 11]. Each of these techniques in spite of its merits will have inherent drawbacks, and cannot fully satisfy characteristics (e.g. highly porous, large-sized pore structure with large interconnection and reasonable mechanical strength) required for a totally accepted scaffolds. For example, the sponge replica technique can give the desired porosity geometry consisting of highly interconnected and large-sized pores. However, the scaffolds resulting from this process generally exhibit insufficient mechanical strength, certainly not enough for load-bearing applications. This is a consequence of the reticulated skeletons which are often cracked during pyrolysis of the polymeric template [5, 7, 12]. Gel casting is used for fabricating ceramic scaffolds with relatively large-sized pores, i.e. of the order of several hundreds of micrometers and also gives high mechanical strength; however, in this case the morphology of pores cannot routinely be achieved by the gel casting [13, 14]. On the other hand, a combined processing route [15] has been introduced to produce highly

T. Y. Yang · J. M. Lee · S. Y. Yoon · H. C. Park (✉)
School of Materials Science and Engineering, Pusan National University, Pusan 609-735, South Korea
e-mail: hcpark1@pusan.ac.kr

porous HA scaffolds with improved mechanical properties, in which a gel casting and polymer sponge method were used simultaneously. After sintering at 1350°C for 2 h, an interconnected porous structure with a pore size of 200–400 μm and a compressive yield strength of ~5 MPa (71% porosity) was obtained; however, any elaborate microstructure control was beyond the capability of this process.

More recently, the freeze casting (drying) process has been proposed to produce porous HA matrix scaffolds with a tailored pore structure, using camphene as a freezing suspension agent. Lee et al. [16] obtained highly porous ceramics with interconnected pore channels by camphene-based freeze casting of 10 vol.% HA slurries. After heating at 1250°C for 3 h, the porosity and compressive strength of the sintered HA materials were 75% and 0.94 MPa, respectively and the pore size (<20 μm in diameter) which formed was too small to enable the material to be used as bone tissue engineering scaffolds. Macchetta et al. [17] fabricated HA/TCP composite scaffolds using a room temperature (4–30°C) camphene-based freeze casting of 10 vol.% solid loading slurry which after sintering at 1280°C for 4 h, gave a porous HA/TCP scaffold with large pore channels containing secondary dendrites. They found that on decreasing the freeze temperature from 30 to 4°C, the compressive strength (for 72.5% porosity, 100–200 μm pore size) increased from 1.95 to 2.98 MPa. These results indicate that the camphene-based freeze casting technique is a more effective process to give special porous structures but it is difficult to produce highly porous tissue engineering scaffolds which have sufficiently large pore size (>200 μm) coincident with desirable mechanical strength.

In the present work, a novel-processing route, i.e. freeze-gel casting combined with polymer sponge technique has been utilized to obtain microstructure-controllable, highly porous HA scaffolds with improved compressive strength, suitable for tissue engineering applications. In this processing route, tertiary-butyl alcohol (TBA) was selected as the freezing component, which can allow for a flexible freezing process and result in relatively long pore channels after sublimation, a consequence of its high freeze temperature (25.3°C) and solidification characteristics particularly its preferential solidification in straight direction [18, 19]. The effects of processing variables (e.g. the slurry concentration, sintering temperature and MgO addition) on crystalline phase, microstructure, physical and mechanical properties of the resulting scaffolds, were investigated.

2 Experimental procedure

2.1 Materials

Commercially available HA powder ($Ca_{10}(PO_4)_6(OH)_2$) (DC Chemical Co., Korea) (Fig. 1) and reagent-grade TBA

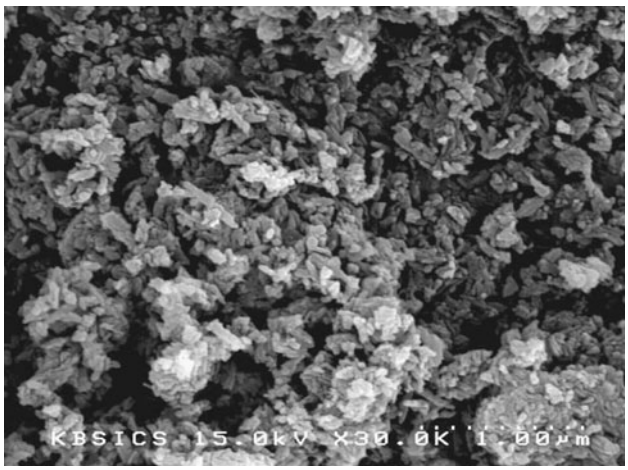

Fig. 1 SEM micrograph of as-received HA powder

($C_4H_{10}O$) (Junsei Chemical Co., Japan) were selected as the bioactive ceramic and the freezing liquid phase, respectively. Magnesium oxide (>99% MgO) (Aldrich Chemical Co., USA) was used as a sintering aid. TBA-based freeze-gel casting slurries were prepared using various processing additives: citric acid (Aldrich Chemical Co., USA) dispersant; ethoxylated acetylenic diol (Dynol 604, Air Products and Chemicals, Inc., USA) surfactant; reactive organic monomer gelators, i.e. mono-functional acrylamide (AM, $C_2H_3CONH_2$, Aldrich Chemical Co., USA) and di-functional *N,N′*-methylenebisacrylamide (MBAM, $(C_2H_3CONH)_2CH_2$, Aldrich Chemical Co., USA); free radical initiator, i.e. ammonium persulphate (APS, $(NH_4)_2S_2O_8$, Kanto Chemical Co., Japan). A flexible polyurethane polymer sponge with the cell size of 75 PPI (pores per linear inch) was used.

2.2 Processing

Schematic illustrations of the TBA-based freeze-gel casting/polymer sponge method for fabrication of microstructure-controllable porous HA scaffolds with high compressive strength are shown in Fig. 2. The freeze-gel casting slurries were prepared at 5, 7.5, 10, and 15 vol.% solid loading by adding HA powder into premixed solution with the weight percent of TBA/AM/MBAM = 90/9.6/0.4; then, 1 wt% citric acid, based on HA powder content and 0.25 wt% Dynol 604, based on monomer solution were then added. To improve their dispersion stability, the slurries were stabilized at a pH of ~3 by adding acetic acid. 1–5 wt% MgO was added in some batches, based on HA content. The prepared slurries were homogenized by ball milling at 30°C for 24 h and then stabilized at 15°C in a water bath to restrict further polymerization of AM (Fig. 2a). After de-airing under vacuum for 3 min, an aqueous solution of 40 wt% initiator, $(NH_4)_2S_2O_8$, was

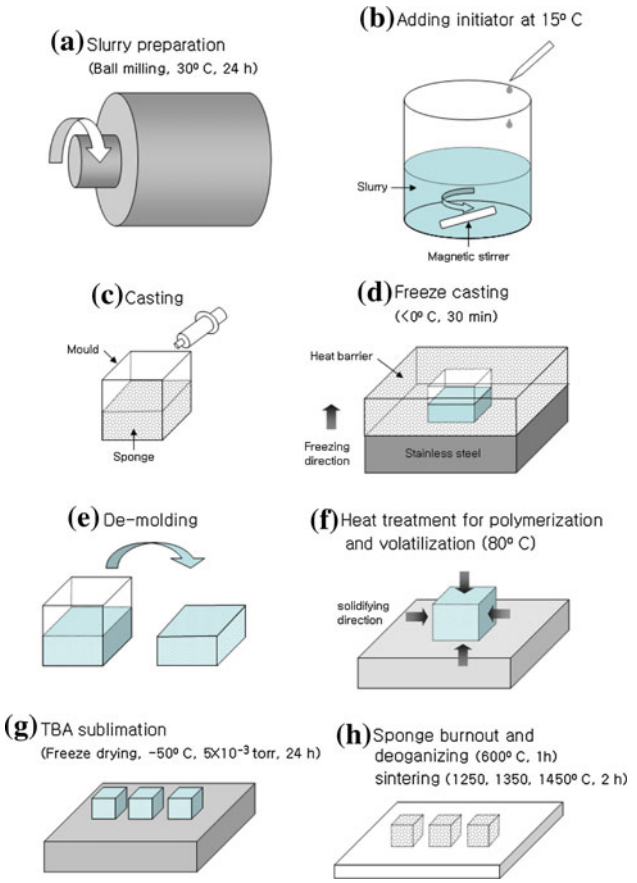

Fig. 2 Processing for fabricating porous HA scaffolds using the TBA-based freeze-gel casting/polymer sponge technique

slowly dropped into the slurries which were continuously stirred using a magnetic stirrer (Fig. 2b). A 20 wt% concentrated solution was used up to 15 vol.% solid loading to control the polymerization rate; the actual amount of initiator added was 3 wt%, based on the monomer content.

Polyurethane foams was cut into a suitable shape and size and placed in a close fit polyethylene mold backed by a heat insulating later in which the bottom face of the mold was tightly capped. The prepared warm HA slurry was then poured into the foam molds (Fig. 2c). To aid complete impregnation the foams were squeezed slightly five times. Subsequently, the mold was placed on a stainless steel plate which was temperature-controlled at <0°C (Fig. 2d). In this condition, controlled freezing of the TBA gradually takes place from bottom to top of the specimen, resulting in unidirectional TBA solidification which on evaporation will give pore channels through the whole cast body. The frozen samples were carefully removed from the molds (Fig. 2e) and then heat-treated at 80°C for 30 min in dry oven for the rapid polymerization of AM with the initiator (Fig. 2f). In the course of this heat treatment stage, the melting and partial evaporating of frozen TBA (boiling point: 82.5°C) will occur. Subsequently, the residual TBA was further

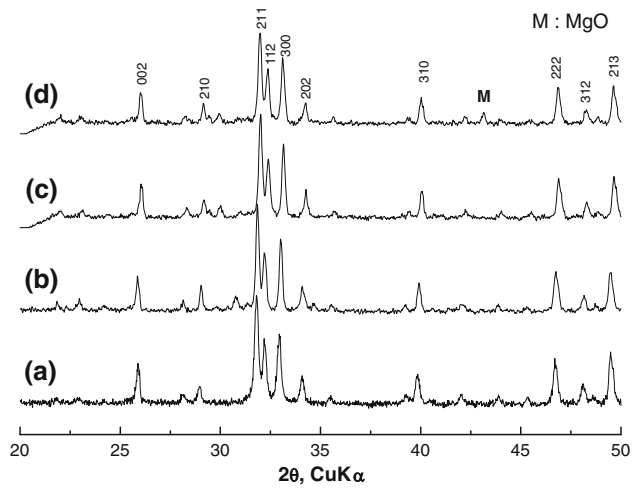

Fig. 3 XRD patterns of *a* as-received HA powder and porous HA scaffolds sintered at *b* 1350°C, *c* 1450°C and *d* 1450°C for 2 h with 3 wt% MgO

sublimated in a freeze drier (Labconco 77540, Western Medics, USA) (Fig. 2g). Both the evaporation and additional sublimation of frozen TBA can result in pore channels. After the sublimation, the samples were given a preliminary calcination at 600°C for 1 h (heating rate: of 1°C/min) to remove organic additives and remnant polyurethane foams. Subsequently the samples were sintered at 1250–1450°C for 2 h (heating rate: 3°C/min) in air (Fig. 2h).

2.3 Characterization

The crystalline phase, morphology, porosity, and mechanical properties of the fabricated porous HA scaffolds were investigated. The crystalline phase was examined using X-ray diffractometry (XRD, D/max-IIA, Rigaku, Japan). The pore and skeleton morphologies were observed using optical microscopy and a scanning electron microscopy (SEM, JSA-840A, Jeol, Japan). The pore size and strut thickness were measured for five specimens sintered at 1350°C using SEM micrographs; then, 15–20 pores and struts were arbitrarily selected in each specimen. The compressive strength was measured for five sintered specimens with dimensions of $\sim 5 \times 5 \times 8$ mm using a Universal Test Machine (model 6025, Instron, USA) with a crosshead speed of 0.5 mm/min and a load cell of 1 kN, and calculated the load at fracture by cross-sectional area. Sintered porosity was measured by the water immersion method.

3 Results and discussion

3.1 Crystalline phases of sintered scaffolds

Several authors [20–23] have reported on the temperature dependency of HA stability; however, there are

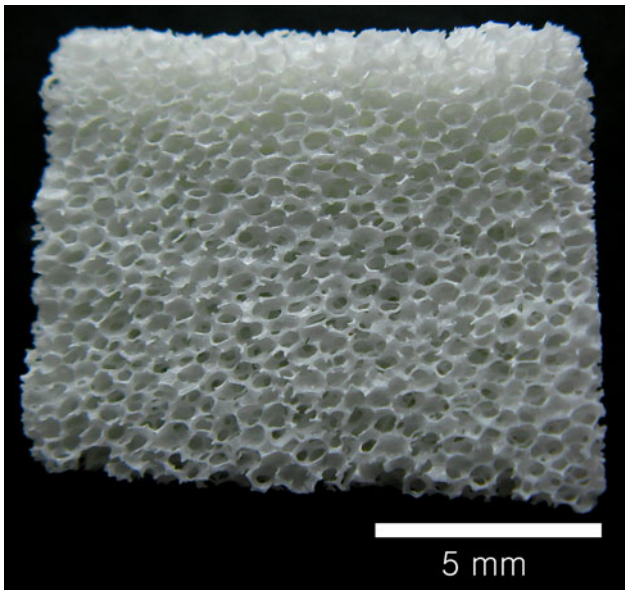

Fig. 4 Optical microphotograph of porous HA scaffold fabricated by the freeze-gel casting/sponge method; sintered at 1450°C for 2 h with 5 wt% MgO and 5 vol.% solid loading

disagreements about the decomposition temperature of HA, the reasons mainly involving different powder characteristics and firing conditions. At >1200°C in air, generally, HA is likely to decompose through gradual loss of OH groups, resulting in tricalcium phosphate (TCP), and tetracalcium phosphate ($Ca_{10}(PO_4)_6(OH)_2 \rightarrow 3Ca_3(PO_4)_2 + CaO + H_2O$) [24]. The presence of other calcium phosphate phases together with HA can change biological properties (cellular response and solubility in human blood); for an example, the solubility of calcium phosphate materials increases in the order of HA $\ll$ β-TCP $<$ α-TCP [25]. Figure 3 shows XRD patterns of as-received HA powder and its sintered scaffolds. During sintering at temperatures up to 1450°C for 2 h, the ceramic exhibited nearly all characteristic peaks corresponding to HA (JCPDS card # 9-432). The peak intensities were somewhat higher with increasing sintering temperature. Similar XRD patterns were also obtained with MgO addition; however, a relatively low peak intensity of the periclase phase was observed for the characteristic (200) diffraction plane (Fig. 3d). These XRD results indicate that it is possible to sinter and densify the scaffolds at temperatures $\leq$1450°C with the ignorable formation of other reaction product calcium phosphate phases except HA.

3.2 Porous structures

The optical micrograph of the sintered HA scaffolds showed that they consisted of interconnected arms and sheets of dense ceramic containing uniformly distributed open pores (Fig. 4). It is also clear that the external macroshape of polyurethane foams was maintained without any structural collapse. Processing variables (e.g. solid loading, sintering temperature, and sintering additive) can play an important role in determining the characteristics (e.g. microstructure, porosity, and mechanical strength) of the

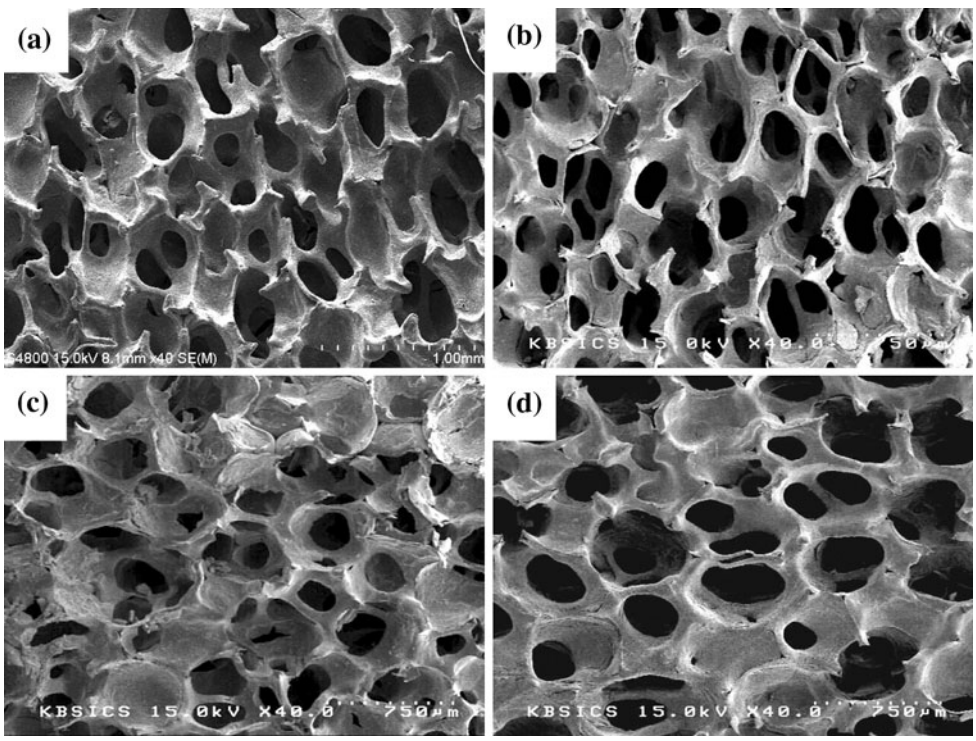

Fig. 5 SEM micrographs of porous HA scaffolds sintered at **a** 1250°C with 15 vol.% solid loading, **b** 1350°C with 10 vol.%, **c** 1450°C with 7.5 vol.% and **d** 1350°C with 10 vol.% and 3 wt% MgO

sintered scaffolds. The effects of solid loading (5–15 vol.%), firing temperature (1250–1450°C), and the addition of a sintering additive (3 wt% MgO) on microstructures of the sintered scaffolds have been examined, and the SEM micrographs are given in Fig. 5. Consequently, similar reticulated structure was obtained. The pore size and the strut thickness were affected by these variables, especially the level of solid loading. The pores were sized in the range 180–360 μm and the struts had a thickness of 38–118 μm. Relatively high deviation in pore size and strut thickness was obtained, presumably due to the partially poor wetting of HA suspension on the sponge and/or inhomogeneous shrinkage of the reticulated structure during sintering at any given temperature. The average pore size was found inversely proportional to the strut thickness (Fig. 6), due to the constant pore cell size and volume, of the starting polyurethane foam. Such a pore structure and pore size can allow osteoblasts to grow into the scaffolds.

After sintering at 1350°C with 10 vol.% solid loading, the microstructures of the struts were examined in detail. The unidirectional pore channels aligned regularly along the growth direction of the frozen TBA crystals and were observed to extend over a long range (Fig. 7a). This morphology differs from the dendritic structure of water- or camphene-based freeze casting which grows in several directions [17, 26]. The growth of the solidified TBA in a straight direction over a considerable length at its freezing temperature may more easily provide a channel for blood supply to the developing connective tissues after sublimation and sintering. At higher magnification (Fig. 7b), the outer walls of the pore channels showed a relatively dense structure containing a few inter-granular, sphere-shaped small pores (<∼2 μm) and inter-agglomerated, longitude-like large pores (<∼10 μm); furthermore, the walls were interconnected with each other. Such a microstructure made up of the continuous scaffolds could give a respected

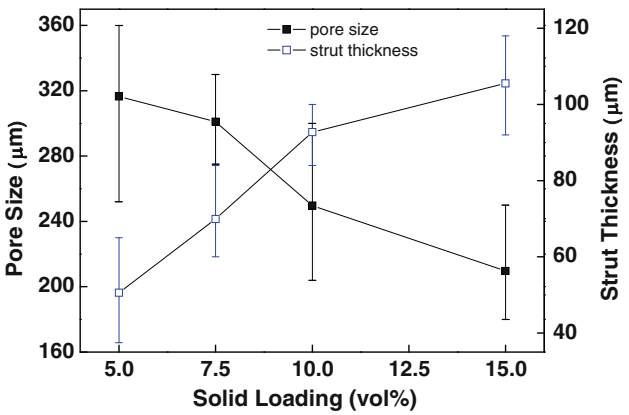

Fig. 6 Pore size and strut thickness of porous HA scaffolds sintered at 1350°C as a function of solid loading

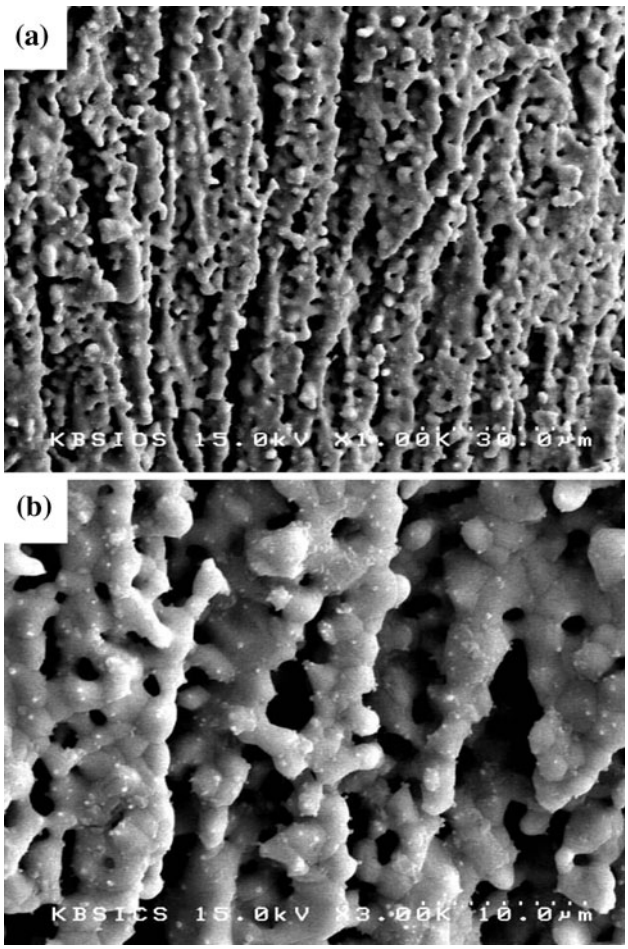

Fig. 7 Microstructures of strut with unidirectional pore channels over the long range, formed by the evaporation of TBA ice

mechanical strength at the same time allowing regrowth mechanisms to take place via the biomimetic porosity.

3.3 Properties of sintered scaffolds

The porosity of porous HA scaffolds fabricated with different solid loadings are shown in Fig. 8. With increasing solid concentration, the porosity (91.1–53.8%) decreased. Consequently, the improved mechanical properties due to the denser and thicker struts (Fig. 5) would be expected with higher solid loading. If this were not the case, the presence of any critical inherent flaws would be likely to result in a reduced strength in the porous scaffolds. The magnesium oxide has been shown to be a good candidate additive for enhancing the sintering of HA. Since in tissue engineering there is a requirement for the HA scaffolds to posses a high porosity(macro) as well as a high strut density(micro) (i.e. to give high mechanical strength), the optimum processing conditions corresponding to a certain specific application for tissue substitution can be selected.

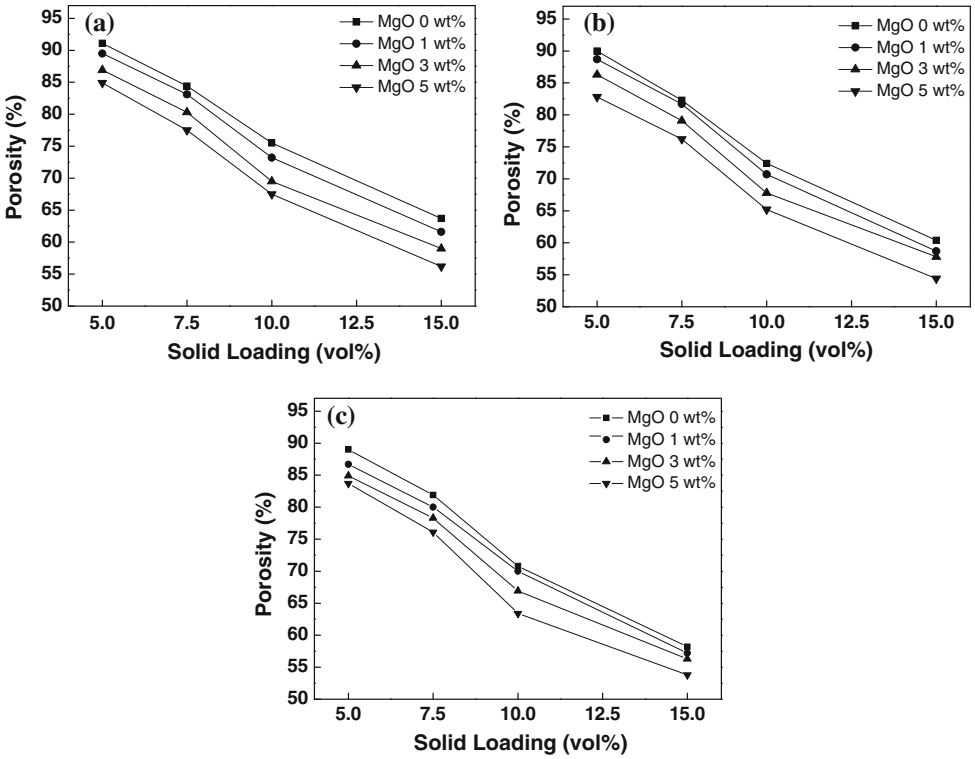

Fig. 8 Apparent porosities of porous HA scaffolds sintered at **a** 1250°C, **b** 1350°C and **c** 1450°C for 2 h as a function of solid loading

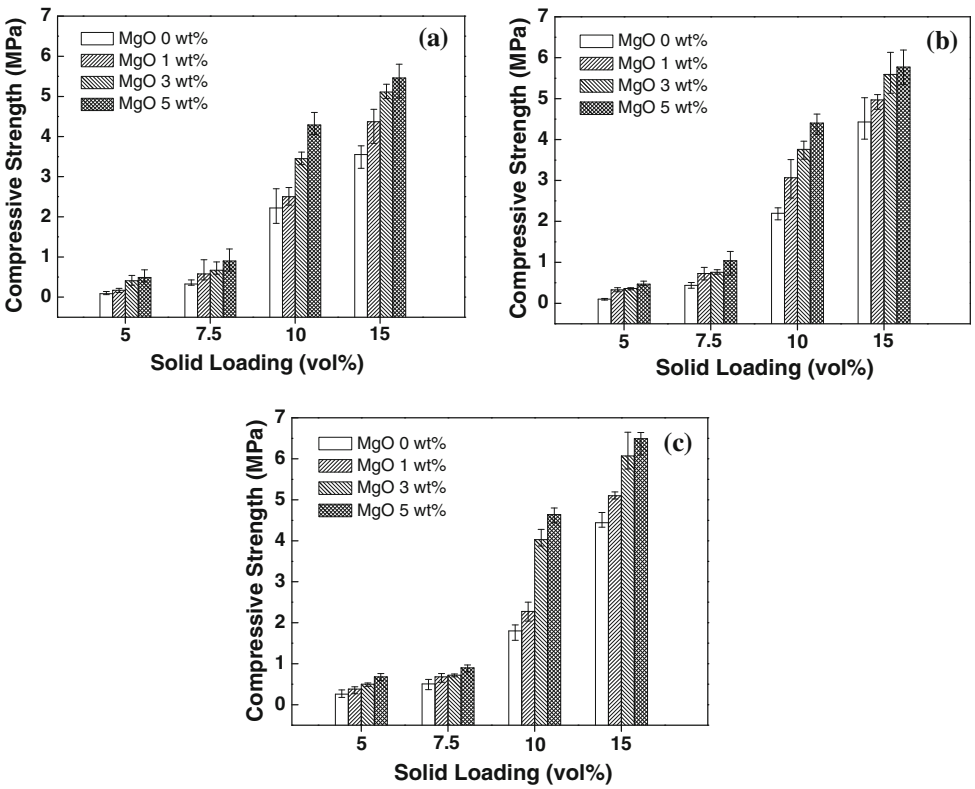

Fig. 9 Compressive strength of porous HA scaffolds sintered at **a** 1250°C, **b** 1350°C and **c** 1450°C for 2 h as a function of solid loading

Figure 9 shows the effect of solid concentration on the compressive strength of porous HA scaffolds. With increasing solid loading, the sintered compressive strength gradually increased. The compressive strength was higher in the scaffolds with MgO addition. It is assumed that this higher strength is partially due to the constrained grain

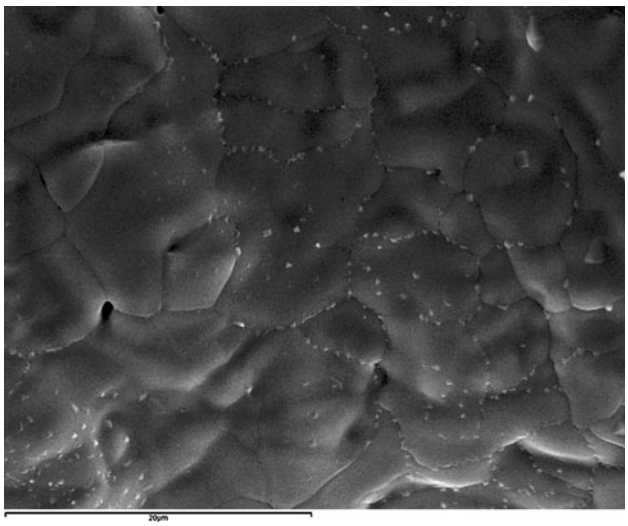

Fig. 10 SEM micrograph of HA scaffold sintered at 1350°C for 2 h with 10 vol.% solid loading and 3 wt% MgO

growth of the matrix phase by the distributed MgO additive particles, which mainly exist at the grain boundaries of HA during sintering (Fig. 10). Especially with 5 wt% MgO addition, relatively high strength values (4.03–6.57 MPa) were obtained in ≥10 vol.%, dependent on the sintering temperature; these attractive strength values were measured in the range 4–12 MPa corresponding to the compressive strength of cancellous bone [27].

4 Conclusions

Highly porous HA scaffolds with controlled pore structure and good compressive strength can be prepared by the new TBA-based freeze-gel casting/polymer sponge technique. The results indicate considerable promise for bone tissue engineering applications. The pore morphology of the scaffolds appears to be tailored by the control available in the freeze casting, gel casting, and polymer sponge route, i.e. a reticulated structure with interconnected, large pores (>∼200 μm in diameter) by the polymer sponge, unidirectional pore channels (∼4.5 μm in diameter) with a long range by TBA-based freeze casting, and a few isolated, small-sized pores (<2 μm) by gel casting. With increasing solids loading from 5 to 15 vol.%, the sintered porosity (91–54%) and pore size (350–198 μm) decreased while the thickness of struts increased in the range 50–106 μm. Consequently, these microstructural properties are partially responsible for the improvement in compressive strength seen with higher solids loading. The presence of a MgO particulate phase appears to contribute to further strengthening, possibly by inhibiting to some extent the grain growth of the matrix phase during sintering. It is suggested that the attractive strength of the scaffolds prepared by this combined technique is mainly due to dense struts obtained by gel casting.

Acknowledgements This work was supported by the Korea Research Foundation Grant funded by the Korean Government (KRF-2008-313-D00459). Also, this study (Dr. Yang) was financially supported by Pusan National University in the program, Post-Doc. 2009.

References

1. Padilla S, Sanchez-Salcedo S, Vallet-Regi M. Bioactive and biocompatible pieces of HA/sol-gel glass mixtures obtained by the gel-casting method. J Biomed Mater Res. 2005;75A:63–72.
2. Cerroni L, Filocamo R, Fabbri M, Piconi C, Caropresso S, Condo SG. Growth of osteoblast like cells on porous hydroxyapatite ceramics: an in vitro study. Biomol Eng. 2002;19:119–24.
3. Hench LL, Wilson J. Surface-active biomaterials. Science. 1984;226:630–6.
4. Komlev VS, Barinov SM. Porous hydroxyapatite ceramics of bi-modal pore size distribution. J Mater Sci Mater Med. 2002; 13:295–9.
5. Jun IK, Song JH, Choi WY, Koh YH, Kim HE. Porous hydroxyapatite scaffolds coated with bioactive apatite-wollastonite glass-ceramics. J Am Ceram Soc. 2007;90:2703–8.
6. Kim HW, Knowles JC, Kim HE. Hydroxyapatite porous scaffold engineered with biological polymer hybrid coating for antibiotic vancomycin release. J Mater Sci Mater Med. 2005;16:189–95.
7. Zhang Y, Zhang M. Three dimensional macroporous calcium phosphate bioceramics with nested chitosan sponges for load bearing bone implants. J Biomed Mater Res. 2002;61:1–8.
8. Zhang FZ, Kato K, Fuji M, Takahashi M. Gelcasting fabrication of porous ceramics using a continuous process. J Eur Ceram Soc. 2006;26:667–71.
9. Sepulveda P. Gelcasting foams for porous ceramics. Am Ceram Soc Bull. 1997;76:61–5.
10. Yook SW, Kim HE, Yoon BH, Soon YM, Koh YH. Improvement of compressive strength of porous hydroxyapatite scaffolds by adding polystyrene to camphene-based slurries. Mater Lett. 2009;63:955–8.
11. Lyckfeldt O, Ferreira JMP. Processing of porous ceramics by starch consolidation. J Eur Ceram Soc. 1998;18:131–40.
12. Studart AR, Gonzenbach UT, Tervoort E, Gauckler LJ. Processing routes to macroporous ceramics: a review. J Am Ceram Soc. 2006;89:1771–89.
13. Chu TMG, Halloran JW, Hollister SJ, Feinberg SE. Hydroxyapatite implants with designed internal architecture. J Mater Sci. 2001;12:471–8.
14. Sepulveda P, Binner JGP, Rogero SO, Higa OZ, Bressiani JC. Production of porous hydroxyapatite by the gel casting of foams and cytotoxic evaluation. J Biomed Mater Res. 2000;50:27–34.
15. Rehman H, Zhang M. Preparation of porous hydrxyapatite scaffolds by combination of the gel- casting and polymer sponge methods. Biomaterials. 2003;24:3293–302.
16. Lee EJ, Koh YH, Yoon BH, Kim HE, Kim HW. Highly porous hydroxyapatite bioceramics with interconnected pore channels using camphene-based freeze casting. Mater Lett. 2007;61: 2270–3.
17. Macchetta A, Turner IG, Bowen CR. Fabrication of HA/TCP scaffolds with a graded and porous structure using a camphene-based freeze-casting method. Acta Biomater. 2009;5:1319–27.
18. Chen R, Wang CA, Huang Y, Ma L, Lin W. Ceramics with special porous structures fabricated by freeze-gelcasting: using

tert-butyl alcohol as a template. J Am Ceram Soc. 2007;90: 3478–84.
19. Chen R, Huang Y, Wang CA, Qi J. Ceramics with ultra-low density fabricated by gelcasting: an unconventional view. J Am Ceram Soc. 2007;90:3424–9.
20. Pramanik S, Agarwal AK, Rai KN, Garg A. Development of high strength hydroxyapatite by solid- state-sintering process. Ceram Inter. 2007;33:419–26.
21. Rodriguez-Lorenzo LM, Vallet-Regi M, Ferreira JMF. Fabrication of hydroxyapatite bodies by uniaxial pressing from a precipitated powder. Biomaterials. 2001;22:583–8.
22. Tampieri A, Gelotti G, Szontagh F, Landi F. Sintering and characterization of HA and TCP bioceramics with control of their strength and phase purity. J Mater Sci Mater Med. 1997;8:29–37.
23. Zhou J, Zhang X, Chen J, De Zeng S, Groot K. High temperature characteristics of synthetic hydroxyapatite. J Mater Sci Mater Med. 1993;4:83–5.
24. Kivrak N, Tas AC. Synthesis of calcium hydroxyapatite-tricalcium phosphate (HA-TCP) composite bioceramic powders and their sintering behavior. J Am Ceram Soc. 1998;81:2245–52.
25. Lin FH, Liao CJ, Chen KS, Sun JS, Lin CP. Petal-like apatite formed on the surface of tricalcium phosphate ceramic after soaking in distilled water. Biomaterials. 2001;22:2981–92.
26. Fukasawa T, Ando M. Synthesis of porous ceramics with complex pore structure by freeze-dry processing. J Am Ceram Soc. 2001;84:230–2.
27. Yang S, Leong KF, Du Z, Chya CK. The design of scaffolds for use in tissue engineering. Part I. Traditional factors. Tissue Eng. 2001;7:679–89.